On Multi-Feature Integration for Deformable Boundary Finding

Amit Chakraborty[†], Marcel Worring[‡] and James S. Duncan[†]
[†]Image Processing and Analysis Group,
Departments of Electrical Engg. and Diag. Radiology, Yale University, New Haven, CT-06520
[‡]Faculty of Mathematics and Comp. Science, Univ. of Amsterdam, Amsterdam

Abstract

Precise segmentation of underlying objects in an image is very important especially for biomedical image analysis. Here, we present an integrated approach for boundary finding using region and curvature information along with the gradient. Unlike the previous methods, where smoothing is enforced by penalizing curvature, here the grey level curvature is used as an extra source of information. However, information fusion may not be useful unless used properly. To address that, we present results that highlight the pros and cons of using the various sources of information and indicate when one should get precedence over the others.

Keywords: *biomedical image analysis, image segmentation, boundary finding, region based segmentation, curvature*

1 Introduction

Segmentation and analysis of underlying structures in an image is of importance in a variety of image analysis and computer vision applications including robot vision, pattern recognition and biomedical image processing. We are especially focussed on the latter area where precise segmentation constitutes an important pre-processing step to such tasks as the registration of images obtained from two modalities, quantitative analysis of anatomical structures, the derivation of priors for image reconstruction in another modality and cardiac motion tracking.

In this work, we aim to introduce an integrated framework to handle the segmentation problem using gradient, region and curvature information. Further, we analyze the strengths and weaknesses of the different types of image derived information and under which circumstances each source of information should be given precedence over the others.

The bulk of the existing work on image segmentation can be typically categorized into two basic approaches [1]. Region based methods like [6] relying on the homogeneity of spatially localized features and other pixel statistics [7] suffer from the problems of poor localization and over-segmentation.

The other group of work uses gradient features. Edge detection [2] and edge detection using anisotropic diffusion [11] suffer from the problems of unwanted and broken edges. To circumvent this, deformable whole boundary methods [13, 14, 8] which rely on the gradient features at a subset of the spatial positions of an image (near an object boundary) has become popular. However, whole boundary methods still suffer from a variety of problems similar to that of edge detection as long as it uses gradient information alone to detect the true boundary. Specifically, whenever the high frequency information in an image is either noisy or is missing, the gradient-based boundary finder tends to drift away from the actual boundary. This problem becomes very acute when the signal to noise ratio (SNR) is low, because the gradient is a derivative process that amplifies noise.

One of the ways to address the problem of a low SNR is through the use of region information. Since this information can be obtained (as in the present case) directly from the raw image data, it is less susceptible to noise than higher order derivatives of the data. Also, it is a more global form of information since image classification is done based on the statistical properties of the different regions in an image unlike the gradient information which only uses the pixel values of a particular site.

Another issue that often plagues the gradient-based boundary-finder is that it often tends to smooth out the sharp corners in an object resulting in large localization error. There are a couple of reasons as to why this happens. First, we emphasize smoothness of the boundary to reduce the effects of noise. The other is that if we consider the boundary to lie at locations where the local pixel wise difference is a maximum, by using a gradient-based boundary finder we are in fact ignoring all the other higher order information. Thus, a sensible way to handle this would be to use higher order information like grey level curvature along with gradient.

All this leads us to consider an integrated approach for boundary finding where besides gradient information, region and curvature information could be used. To be noted is that the use of curvature information here is different from that in for example [8] where smoothness is emphasized by penalizing the curvature of the contour. Here, the grey level curvature is used as an added feature that will actually guide the boundary finder in addition to the gradient information. We also investigate which source of information is important under which circumstance.

2 Image-Derived Features

In this section, we shall briefly describe the methods used to acquire the three different data fields from the original image, all of which will be used in the optimization process.

2.1 Gradient Information

We obtain the gradient image in the traditional way of convolving the original image with the first derivative of the Gaussian kernel as in [13].

2.2 Curvature information

Curvature is a measure for the local deviation from the tangent line [12]. Information about the tangent to the isophote lines (lines of equal grey level intensity) can be obtained through the grey level gradient. But the information about the curvature which is second order feature cannot be obtained through the gradient, which is a first order feature.

When we want to place a boundary separating two regions in a grey level image, what we are interested in is to place the boundary in such a way that the difference between the points on either side of the boundary hits a local maximum. To do that, we must first look at the local structure of the image.

A completely continuous image can be considered as an analytic function $L(\vec{r}) = L(x, y)$, with, $L : \mathcal{R} \times \mathcal{R} \Rightarrow \mathcal{R}$. Locally, we may approximate L by its Taylor series:

$$L(\vec{r} + \vec{dr}) = L(\vec{r}) + \vec{\nabla} L \cdot \vec{dr} + \frac{1}{2}\vec{dr} \cdot H[L] \cdot \vec{dr} + ... \quad (1)$$

with

$$\vec{\nabla} L = \left(\frac{\partial L}{\partial x}, \frac{\partial L}{\partial y}\right); \ H[L] = \begin{pmatrix} L_{xx} & L_{xy} \\ L_{xy} & L_{yy} \end{pmatrix}$$

being respectively the gradient and the Hessian. Now, since we intend to place the boundary at locations where the local pixel-wise difference in the grey level value reaches a maximum, we are interested in points, where

$$L(\vec{r} + \vec{dr}) - L(\vec{r}) = \vec{\nabla} L \cdot \vec{dr} + \frac{1}{2}\vec{dr} \cdot H[L] \cdot \vec{dr} + ... \quad (2)$$

is largest. The first term in the RHS of the above is precisely the gradient term and the second term is the second order term. Substituting from the Hessian, we get,

$$\vec{dr} \cdot H[L] \cdot \vec{dr} = L_{xx} dx^2 + 2L_{xy} dx dy + L_{yy} dy^2 \quad (3)$$

The above is the second fundamental form for curves. Also, we know that curvature is proportional to the second fundamental form [12]. Thus one way of incorporating the second order information along with the gradient information would be to use the curvature. Thus, by the use of the curvature information, we can improve the accuracy of the boundary estimation process, especially when the object has sharp edges or corners. The caution here is that, being a second order feature, it is much more sensitive to noise. Thus for an extremely noisy image this information may be misleading.

2.3 Region Information

The main idea here is to classify a particular image into a number of regions or classes. For our purposes, we choose one that gives reasonable results under most circumstances [9, 10]. It models the image as a Markov Random Field (MRF) and a Maximum *a posteriori* (MAP) probability approach is used to do the classification.

3 Multi-feature Integrated Boundary Finding

In this section we first describe the boundary parameterization used and then discuss the implementation of the integrated boundary finding procedure.

3.1 Boundary Parameterization

We use the approach due to Staib and Duncan [13] which uses a Fourier parameterization which we have adopted in this work as our primary approach.

3.2 Multi-feature Integration

Once, the data has been acquired from the original image in the form of region, gradient and curvature information, our aim here is to combine them using the maximum *a posteriori* framework.

Thus, we want to maximize $P(p|I_g, I_c, I_s)$, where p is the vector of parameters used to parameterize the contour, I_g is the gradient image, I_c is the curvature image, and I_s is the region classified image. It can be shown that this can reduce to:

$$\begin{aligned} \max_p P(p|I_g, I_c, I_s) \quad \propto \quad & \max_p [lnP(p) + lnP(I_g|p) \\ & + lnP(I_c|I_g, p) + lnP(I_s|p)] \quad (4) \end{aligned}$$

The first term on the RHS in equation (4) corresponds to the prior shape term. When it is non-uniform, it biases the model towards a particular range of shapes. However, since there might be other objects in the image, we would always need an initial estimate of the boundary to start the optimization process.

The second term on the RHS in equation (4) is actually the likelihood term which depends on the gradient image. It is a measure of the likelihood of the contour of the described object being the true boundary, given the gradient image. This is expressed in terms of a contour integral where the integral is computed over C_p, the curve described by the boundary $(x(p, t), y(p, t))$. At each point on the contour, the strength of the boundary is evaluated by the magnitude of the gradient at that particular point, given by the gradient image. Thus the likelihood of the whole contour being the true boundary becomes the following line integral (Staib and Duncan [1]) where σ_g^2 is the variance of the underlying noise process for the gradient image:

$$lnP(I_g|p) = \frac{k_1}{\sigma_g^2} \int_{C_p} I_g(x(p, t), y(p, t)) dt \quad (5)$$

As for the third term, it can be treated in exactly the same way as in the case with the gradient term as it gives additional information for local difference in the pixel strength that may not have been captured by the gradient term. This term will be most effective at those places where the gradient information is not particularly strong, yet there is a sharp change in the curve eg. at corner locations.

However, as has already been mentioned, curvature is a second order feature and thus highly susceptible to noise. To avoid the effects of noise and to be able to use it in a more fruitful way, we should emphasize it's importance at those locations where we expect it to play an important role and de-emphasize it at other locations. One way to do it is to weigh the curvature term along the boundary by the curvature of the contour itself. Thus, where the contour curves rapidly, the curvature information is given more importance and vice-versa. Thus,

$$lnP(I_c|I_g,p) = \frac{1}{\sigma_c^2}\int_{C_p}\alpha_2(x(p,t),y(p,t)) \\ I_c(x(p,t),y(p,t))dt \quad (6)$$

In the above, $\alpha_2(x(p,t),y(p,t))$ is the scaled curvature of the contour and $I_c(x(p,t),y(p,t))$ is the curvature image.

The last term in (4), however incorporates the region based information into the boundary finding framework. The underlying assumption for using this information is that we would like the boundary to enclose within it a homogeneous region. It can be shown, that this term can be represented as [4, 3]:

$$lnP(I_s|p) \propto \int\int_{A_p} I_s(x,y)dA \quad (7)$$

However, it is an area integral whereas the gradient and curvature terms are line integrals. We can save a lot of computation by converting the above to a line integral using Greens theorem and the result is as follows.

$$max_p\, P(p|I_g,I_c,I_s) \equiv max_p\,[lnP(p) \\ + \int_{C_p}(K_1\{I_g(x(p,t),y(p,t)) \\ + \alpha_2(x(p,t),y(p,t))I_c(x(p,t),y(p,t))\}\,dt + \\ K_2\{N_s(x(p,t),y(p,t))\frac{\partial x}{\partial t} + M_s(x(p,t),y(p,t))\frac{\partial y}{\partial t}\})dt] \quad (8)$$

where, $M_s(.)$ and $N_s(.)$ can be obtained from I_s as in [4].

While the above gives us a model to combine the different sources of information, how much of what needs to be combined remains an issue. The quantity $\alpha_2(x(p,t),y(p,t))$ controls the relative importance of the curvature term to the gradient term. From our discussion regarding the curvature term, it is clear that under high SNR conditions it could be as important as the gradient term. Hence, it should have a maximum value of unity. The relationship between K_1 and K_2 controls the relative importance of the derivative and region information. We shall have more to say about this in the discussion and the appendix.

Optimization of the above is achieved using the conjugate gradient method.

4 Results

First, we shall consider the importance of using gray level curvature. An example is shown in Figure 1. As we can see, the contrast is low. The SNR for this image is 3.0. Clearly, the integrated method does a much better job. As expected, the difference is prominent where there are sharper features, i.e. at the location of the peaks.

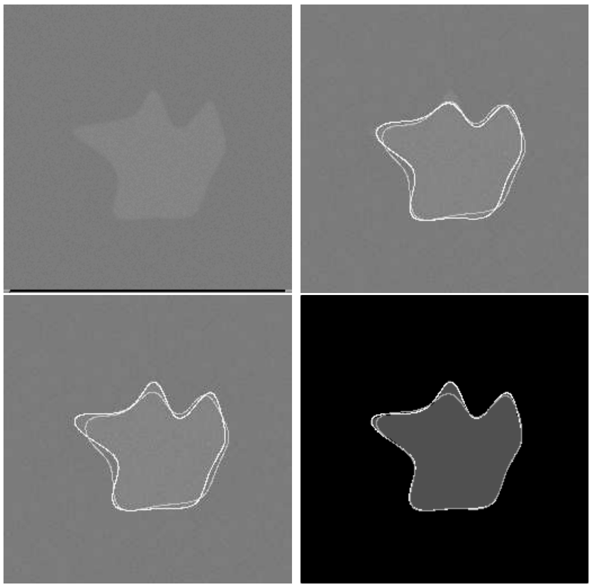

Figure 1: Example with a synthetic image to show the importance of integrating curvature information into the boundary finding framework along with gradient information. For this image, the $SNR = 3.0$, but the contrast is low. (a)Top, Left: The original image; (b)Top, Right: Output of boundary finding using gradient information only. The darker contour represents the initialization, the brighter one the final output. (c)Bottom, Left: Output of boundary finding using gradient and curvature information. The darker contour represents the initialization, the brighter one the final output. (d)Bottom, Right: The outputs overlayed on the template of the object out of which the noisy image was generated. The brighter contour is the one generated using both gradient and curvature information and the darker contour is the one generated by using just the gradient. The output using gradient and curvature is superior to the gradient-based boundary finder (shown by the darker contour) wherever the object curves sharply.

In the next example, we continue with the same object but drastically reduce the SNR. For this image shown in Figure 2, it is profitable to use the region information. This is especially true if as in this case, the size of the object is not negligible. Curvature information is not used due to the extremely low SNR. Use of gradient information alone, results in divergence. On the other hand, if we use both the region and the gradient information as shown we get a decent output.

To further verify the circumstances under which a particular information should be used, we formulated experiments similar to [4, 3] where under the same initialization, the distance between the final output and the true contour was compared under different circumstances and under different situations of information fusion.

It is obvious from Figure 3(a) that in general, integration improves the performance of the boundary finding procedure. When the contrast is high, curvature along

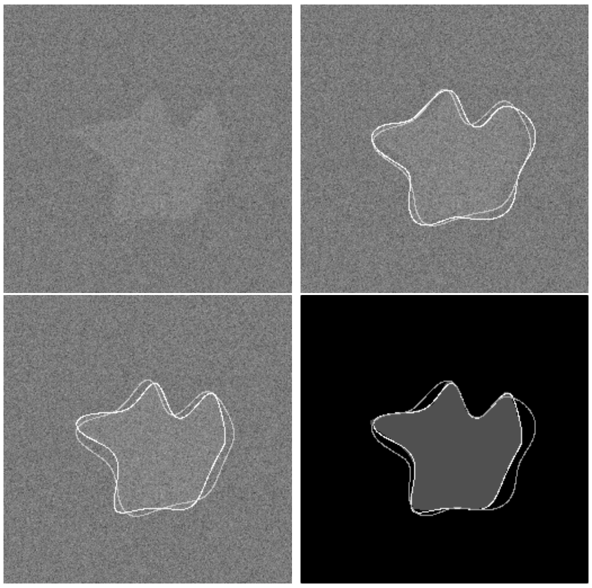

Figure 2: Example with a synthetic image to show the importance of integrating region information into the boundary finding framework along with gradient information. For this image, we have a very low $SNR = \frac{1}{3}$. (a)Top, Left: The original image; (b)Top, Right: Output of boundary finding using gradient information only. The darker contour represents the initialization, the brighter one the final output. (c)Bottom, Left: Output of boundary finding using gradient and curvature information. (d)Bottom, Right: The outputs overlayed on the template of the object out of which the noisy image was generated. The brighter contour is the one generated using both gradient and region information. That it is superior to the gradient-based boundary finder (which diverges and is shown by the darker contour) is evident.

with gradient is almost as good as everything combined. However, as the contrast goes down, both gradient and curvature information degrades and thus the gradient and region combined betters both gradient only and gradient along with curvature. This is due to the more robust nature of the region information as it is not a derivative feature. Obviously, the combined method is in general the preferred one.

From Figure 3(b), we observe that some form of information fusion is always good. As we would expect, however, performance of all the methods deteriorate with increasing noise. The integrated method which combines all three sources of information does better for most part, except when the noise is too large when due to the unreliable curvature information, it starts performing worse than without it i.e., than the gradient and region only case.

In the following example we consider the case of outlining the endocardium of the heart. Figure 4(a) shows a short axis MR image of a canine heart. From our experience this is one of the most difficult images of its type. The superiority of the integrated method is clear.

In the final example, we take up the case of an ultra-

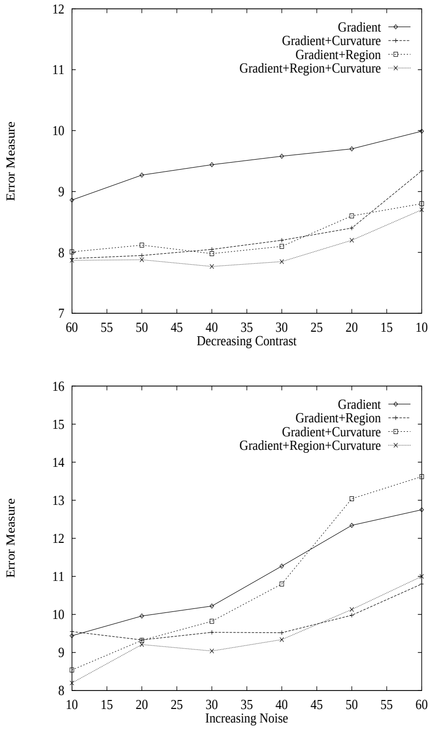

Figure 3: Performance under varying noise and contrast conditions. (Explanations are given in the results section of the text.)

sound image of the heart as shown in Figure 5(a), and the task is to outline the left ventricle. This is an ideal example where the grey level gradient does not mean much. Thus, as shown in Figure 5(b), using a gradient based boundary finder leads us to nowhere. Here, we gave the region term three times the weightage of the gradient term. The region information was derived using a texture segmentation procedure like the one in [10]. It is exactly the same as the algorithm described earlier in this paper, with the only difference being that here we use besides the mean, other higher order statistics. Clearly, the boundary finder in this integrated case does not diverge and the result if not accurate looks reasonable.

5 Discussion

In the section in which we described the integration method, and again in the results section, we pointed out the significance of the fact that while information fusion is helpful in general, it needs to be done appropriately. This is so as there might be cases (as we have already seen) where a source of information may be much more reliable than others and vice versa.

While the relation between the gradient and the curvature information is clear, the relationship between the region and the derivative information (gradient and curvature) is not so obvious. From the brief analysis of the equivalent 1D problem is given in the appendix we observe the following:

1. As we increase the amount of smoothing, for a gra-

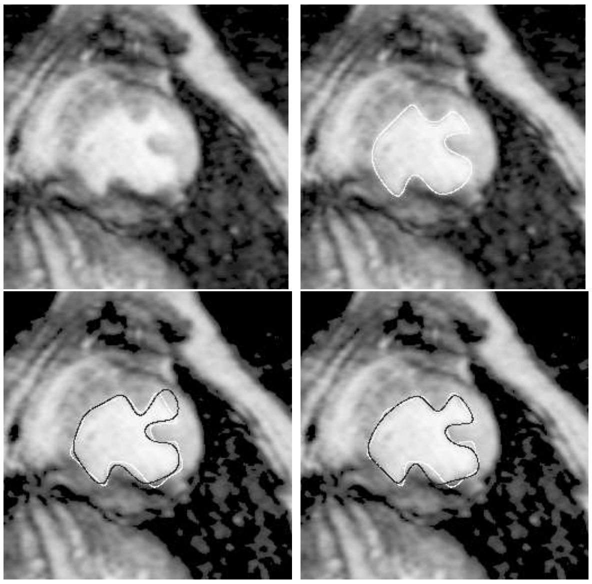

Figure 4: Example with a short axis MR image of a canine heart. (a)Top, Left: Original image; (b)Top, Right: Original image with the contour of the endocardium drawn by an expert; (c)Bottom, Left: Output of Boundary finding using gradient information only. It seems to be diverging; (d)Bottom, Right: Output of Boundary finding using an integrated (gradient + region + curvature) approach using the same initialization. The output looks reasonable. In both (c) and (d), the white contour is the initialization, and the black one is the final output. The superior output in (d) is due to the use of additional features as compared to that in (c). The use of region information helps it to converge. The use of the curvature information helps to keep the boundary sharp.

dient based boundary finder, the SNR (eq. (15)) improves, but the localization error (eq. (11)) increases.

On the other hand, for the region based boundary finding (see equations (14), (16) in the appendix), we note that there is no such tradeoff. Thus if the noise is very high, unlike in the previous case, here it is possible to get good localization.
2. As for the SNR, for gradient based boundary finding, a higher SNR necessarily means poor localization. On the other hand, the SNR from the region based method (16) is proportional to $\sqrt{L}/2$ where L is the size of the region. Thus, in general the SNR in this case would be much larger than the gradient based method.

Thus we might infer based on both the 1D analytical results and the experimental results that for an integrated framework, we should do the following,
(i) If the image has an high SNR, we should emphasize the gradient information over the region information to take advantage of the low localization error of the gradient information.
(ii) If the initialization is far away, or if the SNR is low, we should emphasize the region information to avoid false boundaries or divergence.

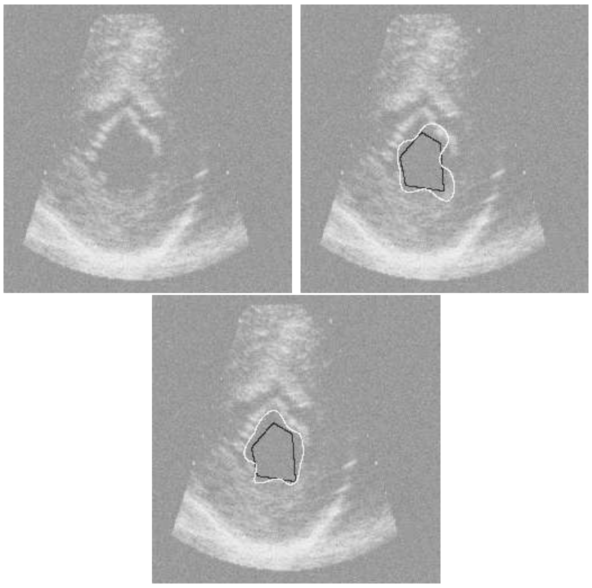

Figure 5: Example with an ultrasound image of the heart. (a)Top, Left: Original image; (b)Top, Right: Output of a gradient based boundary finder. The smaller darker contour is the initialization, and the brighter contour is the final output. That it diverges is clear; (c)Bottom: Output of an integrated (gardient + region) boundary finder which looks quiet reasonable. The brighter one is the final output and the darker one the initialization.

(iii) Even though at this point we are not in a position to exactly quantify the weightings for the different terms, a reasonable weighting scheme would be to use $K_1 = 1$ and $K_2 = 1/SNR$ in equation (8) i.e. give more weight to the region based term as the noise increases. We are presently working for a better scheme that could automatically determine the weightings.

6 Conclusions

We have, presented in this paper a novel method to integrate into the deformable boundary finding framework region and curvature information along with the gradient information. We would like to point out that unlike the previous methods, [8] where low curvature is rewarded to emphasize smoothness of the resulting contour, here the grey level curvature in the image is used as an added source of information to enhance the performance of the boundary finding procedure. The results and the analysis show that the integrated method, when used judiciously, improves the performance of the boundary finder. This is obvious from the results presented both with the synthetic and clinical images.

References

[1] D. H. Ballard and C. M. Brown. *Computer Vision.* Prentice Hall, Englewood Cliffs, 1982.

[2] J.F. Canny. A computational approach to edge-detection. *IEEE Transactions on Pattern Analysis and Machine Intelligence*, 8:679–698, 1986.

[3] A. Chakraborty, L.H. Staib, and J.S. Duncan. Deformable boundary finding influenced by region homogeneity. *Proc. Computer Vision and Pattern Recognition*, pages 624–627, 1994.

[4] A. Chakraborty, L.H. Staib, and J.S. Duncan. An integrated approach to boundary finding in medical images. *Proc. IEEE Workshop on Biomedical Image Analysis*, pages 13–22, 1994.

[5] Amit Chakraborty. *Image Segmentation through Feature Integration.* PhD thesis, Yale University, in preparation.

[6] K.S. Fu and J.K. Mui. A survey of image segmentation. *Pattern Recognition*, 13:3–16, 1981.

[7] D. Geman and S. Geman. Stochastic relaxation, gibbs distribution and bayesian restoration of images. *IEEE Transactions on Pattern Analysis and Machine Intelligence*, 6:721–741, 1984.

[8] M. Kass, A. Witkin, and D. Terzopoulus. Snakes: Active contour models. *International Journal of Computer Vision*, 1:312–331, 1988.

[9] R. Leahy, T. Herbet, and R. Lee. Application of markov random fields in medical imaging. *Information Processing in Medical Imaging*, pages 1–14, 1989.

[10] B.S. Manjunath and R. Chellappa. Unsupervised texture segmentation using markov random field models. *IEEE Transactions on Pattern Analysis and Machine Intelligence*, 13:478–482, 1991.

[11] P. Perona and J. Malik. Scale-space and edge detection using anisotropic diffussion. *IEEE Transactions on Pattern Analysis and Machine Intelligence*, 12:629–639, 1990.

[12] M. Spivak. *A Comprehensive Introduction to Differential Geometry.* Publish or Perish, Berkley, CA, 1970.

[13] L.H. Staib and J.S. Duncan. Boundary finding with parametrically deformable models. *IEEE Transactions on Pattern Analysis and Machine Intelligence*, 14:161–175, 1992.

[14] M. Worring, A.W.M. Smeulders, L.H. Staib, and J.S. Duncan. Parametrized feasible boundaries in gradient vector fields. *Information Processing in Medical Imaging*, pages 48–61, 1993.

Appendix

As mentioned in the Discussion section, we shall model the received edge as:

$$r(x) = I\Phi(\frac{x-l}{\sigma_s}) + n(x) \tag{9}$$

where I is the intensity of the edge, l is the location of it, and σ_s is the amount of blur and Φ is the step response of a Gaussian. We assume that L is the extent of the image, i.e. $x \in [0, L]$. The noise is Gaussian distributed with std. deviation σ_n.

Localization

a) Gradient Based: If we assume (without loss of generality) that the edge is located at $l = 0$, then the error is given by the estimate $\hat{l}$. Without going into the details (see [5] for details), it can be shown, that the mean and the variance of $\hat{l}$ is given by:

$$E(\hat{l}) = 0 \tag{10}$$

$$Var(\hat{l}) = \frac{\sigma_n^2}{I^2}\frac{3\sqrt{\pi}}{4\sigma_c^5}(\sigma_s^2 + \sigma_c^2)^3 \tag{11}$$

b) Region Based: Since we are looking to place the boundary to differentiate homogeneous regions, the boundary should be placed such that the following is satisfied (see [5] for details).

$$\arg\max_l \int_l^L (r(x) - I/2)dx \tag{12}$$

Once again it can be shown that the mean and the variance which is also the localization error for this expression is given by:

$$E(\hat{l}) = 0 \tag{13}$$

and

$$Var(\hat{l}) = 2\pi\sigma_s^2\frac{\sigma_n^2}{I^2} \tag{14}$$

Signal to Noise Ratio

We will once again assume the same model that we started with along with the assumption that the true step is located at the origin

a) Gradient Based:
It can be shown, the SNR is given by:

$$SNR = \sqrt{\frac{S}{N}} = \frac{I}{\sigma_n}\frac{\sqrt{2}}{\pi^{\frac{1}{4}}}\frac{\sigma_c^{\frac{3}{2}}}{(\sigma_c^2 + \sigma_s^2)^{\frac{1}{2}}} \tag{15}$$

b) Region Based:
It can be shown that assuming $L >> \sigma_s$ is true, the SNR is given by:

$$SNR = \sqrt{\frac{S}{N}} = \frac{I}{\sigma_n}\left(\frac{\sqrt{L}}{2} - \frac{\sigma_s}{\sqrt{2\pi L}}\right) \approx \frac{I\sqrt{L}}{2\sigma_n} \tag{16}$$